(25) J. Ahmed and J. A. Ibers, *Inorg. Chem.*, **16**, 935 (1977).
(26) D. De Filippo, P. Deplano, A. Diaz, and E. F. Trogu, *Inorg. Chim. Acta*, **17**, 139 (1976).
(27) (a) M. Cox, J. Darken, B. W. Fitzsimmons, A. W. Smith, L. F. Larkworthy, and K. A. Rogers, *J. Chem. Soc., Dalton Trans.*, 1191 (1972); (b) B. F. Hoskin and C. D. Panna, *Inorg. Nucl. Chem. Lett.*, **11**, 409 (1975).
(28) C. K. Jorgensen, *Adv. Chem. Phys.*, **8**, 47 (1965), and references therein.
(29) R. J. Butcher and E. Sinn, *J. Am. Chem. Soc.*, **98**, 2440, 5159 (1976).
(30) E. Sinn and L. J. Wilson, to be submitted for publication.
(31) G. M. Bancroft, A. G. Maddock, W. K. Ong, R. H. Prince, and A. J. Stone, *J. Chem. Soc. A*, 1966 (1967).
(32) R. M. Housley and H. de Waard, *Phys. Lett.*, **21**, 90 (1966).
(33) N. N. Greenwood and T. C. Gibbs, "Mössbauer Spectroscopy", Chapman and Hall, London, 1971, p 63.
(34) The characteristic time of measurement in Mössbauer spectroscopy is the mean lifetime of the excited Mössbauer level: $\tau(ex) = 1.4 \times 10^{-7}$ s (or 140 ns) in the ^{57}Fe case. If the time of spin conversion between the ls and hs spin states is comparable to the lifetime, τ(spin state) $\gtrsim \tau$(ex), two Mössbauer spectra representing both hs and ls states will be observed. On the other hand, if the spin conversion time is much shorter than the transition time, τ(spin state) $\ll \tau$(ex), an "averaged" spectrum should be observed.
(35) H. C. Stynes and J. A. Ibers, *Inorg. Chem.*, **10**, 2304 (1971).
(36) E. V. Dose, M. A. Hoselton, N. Sutin, M. F. Tweedle, and L. J. Wilson, *J. Am. Chem. Soc.*, in press.
(37) See, for example, ref 10.
(38) S. S. Brody, *Rev. Sci. Instrum.*, **28**, 1021 (1957); D. H. Cooper, *ibid.*, **37**, 1407 (1966).
(39) J. N. Demas and G. A. Crosby, *Anal. Chem.*, **42**, 1010 (1970).
(40) Fundamental limitation on the resolution obtainable in these *T*-jump experiments arises from (1) the duration of the heating pulse (~25 ns), (2) the enthalpy change ($\Delta H°$) associated with the spin transition, and (3) the differences in the molar absorptivities of the hs and ls complexes. The first limitation can be overcome using the method of moments deconvolution approach.[15] The last two limitations decrease the signal-to-noise ratio (Figure 6) but, in general, it has been found possible to optimize the detection system so that these are also not limiting factors.

Contribution from the Department of Chemistry,
William Marsh Rice University, Houston, Texas 77001

Solution-State Spin-Equilibrium Properties of the Tris[2-(2-pyridyl)imidazole]iron(II) and Tris[2-(2-pyridyl)benzimidazole]iron(II) Cations

KAREN A. REEDER,[1] ERIC V. DOSE,[2] and LON J. WILSON*

Received August 3, 1977

Contrary to previous reports, the tris[2-(2-pyridyl)imidazole]iron(II) ($[Fe((py)imH)_3]^{2+}$) and tris[2-(2-pyridyl)benzimidazole]iron(II) ($[Fe((py)bimH)_3]^{2+}$) cations have been shown to be

$$^1A(S=0) \underset{k_{-1}}{\overset{k_1}{\rightleftharpoons}} {}^5T(S=2)$$

spin-equilibrium species in *solution* by variable-temperature magnetic and electronic spectral studies. Laser Raman temperature-jump kinetics has been used to directly measure the forward ($k_1 = 1.1 \times 10^7$ s^{-1}) and reverse ($k_{-1} = 1.0 \times 10^7$ s^{-1}) intersystem crossing rate constants for the *dynamic* spin-interconversion process in $[Fe((py)imH)_3]^{2+}$. The results are compared to similar kinetic data available for other iron(II) spin-forbidden/conversion processes in bis(pyrazolylborate)iron(II) and $[Fe(6\text{-}Mepy)_n(py)_m tren]^{2+}$.

Transition-metal complexes exhibiting anomalous magnetic properties arising from a thermally dependent "spin-equilibrium" between low-spin (ls) and high-spin (hs) states have been studied extensively over the almost 50 years since the phenomenon was first discovered,[3] but such studies have been largely confined to the solid state. Work done on many such compounds, especially the $^1A(ls) \rightleftarrows {}^5T(hs)$ iron(II) complexes of 2-(2-pyridyl)imidazole, $[Fe((py)imH)_3]^{2+}$ (Figure 1), and 2-(2-pyridyl)benzimidazole, $[Fe((py)bimH)_3]^{2+}$, have been hindered by the lack of understanding to date of unpredictable lattice effects arising from various degrees of hydration/solvation, anion change, and possibly *inter*molecular metal–metal magnetic exchange interactions. In particular, studies of these two iron(II) spin-equilibrium systems have been in disagreement in many instances, most likely due to varying methods of preparation and purification which have yielded different solvates, degrees of solvation, and perhaps even different crystal forms of the same solvate.[4,5] In solution, all such generally troublesome effects are eliminated or at least minimized. With this realization, we have recently been engaged in a systematic study of spin-equilibrium phenomena in the solution phase. Furthermore, solution-phase studies provide an important advantage over those in the solid state in that rapid perturbation (*T*-jump) kinetics can be employed[6-14] to directly measure first-order rate constants k_1

$$\text{low spin} \underset{k_{-1}}{\overset{k_1}{\rightleftharpoons}} \text{high spin} \qquad (1)$$

and k_{-1} for *dynamic* spin-interconversion (intersystem crossing) processes. Such studies are of fundamental importance in understanding intersystem crossing phenomena as they relate to photochemically induced excited states[15] and for a general understanding of the role of spin-multiplicity changes on electron-transfer rates.[16]

In this work we report the solution-state spin-equilibrium properties for the $[Fe((py)imH)_3]^{2+}$ and $[Fe((py)bimH)_3]^{2+}$ cations, both of which have been found to exhibit the phenomenon in solution contrary to earlier findings.[17,18] In addition, the neutral iron(III) complex of the 2-(2-pyridyl)imidazolate anion, $Fe((py)im)_3$, has also been prepared by deprotonation of $[Fe((py)imH)_3]^{2+}$, via an $Fe((py)imH)_2Cl_2$ intermediate, and characterized as low spin in both the solution and solid states.

Experimental Section

Materials. Reagent grade $FeCl_2 \cdot 4H_2O$ was obtained commercially. Reagent grade pyridine-2-carboxaldehyde from Aldrich was freshly distilled before use. All other reagents, including the 2-(2-pyridyl)benzimidazole ligand (Aldrich) were reagent grade and were used without further purification.

Physical Measurements. Magnetic measurements in solution were performed by the Evans ^1H NMR method[19] using methanol for temperature calibration. A first-order correction for changes in solvent density and sample concentration was employed.[20] UV–vis spectra were run on a Cary 17 instrument using jacketed, insulated quartz cells; reported temperatures are ±0.5 °C and were monitored with a thermistor. Solution conductivities in acetone and methanol were obtained with a Model 31 YSI conductivity bridge. Elemental analyses were performed commerically. Mass spectra were obtained on a Finnigan Model 9500 GC/MS.

0020-1669/78/1317-1071$01.00/0

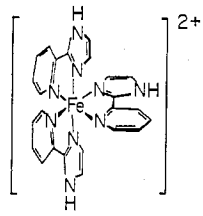

Figure 1. Schematic structure of the tris[2-(2-pyridyl)imidazole]-iron(II) cation as the *mer* isomer.

The temperature-jump experiments were performed using the laser-stimulated Raman system previously described.[21] For these experiments, sample cells with 20-μm path lengths were employed and sample solutions of about 3×10^{-3} M $[Fe((py)imH)_3](BPh_4)_2$ in CH_3CN (20%)/CH_3OH were used. The experiments were conducted at sample temperatures of +23 and −2 °C. Equilibrium constants $K_{eq} = [hs]/[ls] = k_1/k_{-1}$ for the intersystem-crossing

$$^1A(Fe^{2+}, ls) \underset{k_{-1}}{\overset{k_1}{\rightleftharpoons}} {}^5T(Fe^{2+}, hs)$$

processes were obtained from the magnetic susceptibility measurements with the values used being 1.06 at 23 °C and 0.59 at −2 °C. Rate constants k_1 and k_{-1} were calculated from the measured first-order relaxation times of $\tau = 48$ ns at 23 °C and $\tau = 45$ ns at −2 °C and the equilibrium constant, using the relationship $\tau^{-1} = k_1 + k_{-1}$. The spin-state lifetimes $\tau(^1A)$ and $\tau(^5T)$ are then k_1^{-1} and k_{-1}^{-1}, respectively.

Syntheses. 2-(2-Pyridyl)imidazole, (py)imH. The ligand was synthesized by modification of the preparation due to Radziszewski.[22] A solution of 20 g (190 mmol) of pyridine-2-carboxaldehyde and 20 mL of 95% ethanol was cooled to 0 °C and added to a solution of 27 mL of 40% aqueous glyoxal in 20 mL of 95% ethanol, also at 0 °C. The mixture was stirred in an ice bath, and 64 mL of cold aqueous NH_3 (30%) was added as quickly as possible while maintaining the temperature of the entire mixture below about 5 °C. The stirring solution gradually turned brown and was allowed to warm to room temperature after 1 h. The volume was reduced by gentle warming under vacuum, and the remaining solution was extracted several times with ethyl ether. The ether extracts were combined and dried thoroughly (Na_2SO_4), and the ether was removed under vacuum to yield a brown oil which was distilled under vacuum. The clear yellow oil so obtained solidified and was recrystallized from ethyl acetate, yielding 9 g (33%) of light yellow needles, mp 136 °C (uncor).

Tris[2-(2-pyridyl)imidazole]iron(II) Tetraphenylborate Monohydrate Carbon Tetrachloride Solvate, $[Fe((py)imH)_3](BPh_4)_2 \cdot CCl_4 \cdot H_2O$. Two grams (13.8 mmol) of 2-(2-pyridyl)imidazole ((py)imH) was dissolved in 40 mL of methanol and the mixture was stirred. Upon addition of 0.91 g (4.6 mmol) of $FeCl_2 \cdot 4H_2O$, the solution turned dark red. After 15 min of stirring, a solution of 7.07 g (20.6 mmol) of $NaBPh_4$ in 30 mL of methanol was filtered and added dropwise with stirring. The red-orange precipitate was collected, washed with large volumes of water and then methanol, and extracted into dry CH_2Cl_2 (Soxhlet). The dark red extract was concentrated under vacuum, and subsequent dropwise addition of dry CCl_4 produced a dark red material which was collected, washed with cold CCl_4, and dried in vacuo over P_2O_5 at room temperature for 24 h yielding 1.6 g (27%) of a red powder. Anal. Calcd for $FeC_{73}H_{60}N_9OB_2Cl_4$: C, 67.38; H, 4.65; Fe, 4.30; N, 9.69. Found: C, 67.40; H, 4.75; Fe, 4.48; N, 9.89. $\Lambda_c = 148$ $\mu\Omega^{-1}$ cm^{-1} at 30 °C and 10^{-3} M in acetone; μ_{298}(solid) = 2.23 μ_B.

Tris[2-(2-pyridyl)benzimidazole]iron(II) Tetraphenylborate Trihydrate, $[Fe((py)bimH)_3](BPh_4)_2 \cdot 3H_2O$. A solution of 0.68 g (3.4 mmol) of $FeCl_2 \cdot 4H_2O$ in 10 mL of methanol was added to a stirring solution of 2.0 g (10.2 mmol) of 2-(2-pyridyl)benzimidazole((py)bimH) in about 20 mL of methanol. To this red solution was added dropwise a filtered solution of 2.5 g (7.3 mmol) of $NaBPh_4$ in 10 mL of methanol, and the precipitate thus formed was collected and washed with methanol and then with ethyl ether. The dark orange powder was suspended in water and the mixture was stirred for 1 h. The powder was then collected, washed with water, methanol, and ethyl ether, and air-dried. The product was dried in vacuo over P_2O_5 at room temperature for 9 h, yielding 4.3 g (94%) of an orange powder. Anal. Calcd for $FeC_{84}H_{73}N_9O_3B_2$: C, 75.63; H, 5.52; Fe, 4.18; N, 9.45. Found: C, 75.28; H, 5.35; Fe, 4.05; N, 9.28. $\Lambda_c = 173$ $\mu\Omega^{-1}$ cm^{-1} at 30 °C and 10^{-3} M in acetone and 131 $\mu\Omega^{-1}$ cm^{-1} at 30 °C and 10^{-3} M in methanol; μ_{298}(solid) = 5.07 μ_B. (Drying at 117 °C in vacuo over P_2O_5 for 9 h yielded a product whose analysis corresponds to the anhydrous complex. Calcd for $FeC_{84}H_{67}N_9B_2$: C, 78.66; H, 5.27; Fe, 4.56; N, 9.83. Found: C, 78.21; H, 5.15; Fe, 4.35; N, 10.02.)

Tris[2-(2-pyridyl)imidazolato]iron(III) Sesquihydrate, $[Fe((py)im)_3] \cdot 1.5H_2O$. Six grams (5.3 mmol) of $[Fe((py)imH)_3](BPh_4)_2 \cdot CCl_4 \cdot H_2O$ was dissolved in 50 mL of acetone. The mixture was filtered and added dropwise into a filtered, stirring solution of 0.46 g (10.8 mmol) of LiCl in 150 mL of acetone. The precipitate was collected, rinsed with acetone and then with ethyl ether, and air-dried. The elemental analysis of this intermediate yielded an empirical formula $FeC_{15.9}H_{14.6}N_6Cl_{2.1}$ corresponding closely to $FeC_{16}H_{14}N_6Cl_2$ as expected for $Fe((py)imH)_2Cl_2$. The solid (about 2 g) was dissolved in 800 mL of methanol to which 0.56 g (10.4 mmol) of $NaOCH_3$ in 400 mL of methanol was added over 9 h. The solution became dark purple and the solvent was removed under vacuum. The solid thus obtained was extracted, with some difficulty, into dry CH_2Cl_2, the extract was filtered, and an equivalent volume of CCl_4 was added. The CH_2Cl_2 was removed under vacuum with gentle heat and the solution filtered. The remaining solvent was then removed under vacuum and the resulting green solid collected. The solid was dried at room temperature in vacuo over P_2O_5, yielding 0.25 g (9%) of green crystals. Anal. Calcd for $FeC_{24}H_{21}N_9O_{1.5}$: C, 55.94; H, 4.11; N, 24.46; Fe, 10.84. Found: C, 55.92; H, 4.06; N, 24.66; Fe, 10.52. $\Lambda_c = 4.9$ $\mu\Omega^{-1}$ cm^{-1} at 10^{-3} M in methanol and 30 °C; μ_{298}(solid) = 2.01 μ_B.

Solution-State Magnetic Data (T in K, μ_{eff} in μ_B). $[Fe((py)imH)_3](BPh_4)_2 \cdot CCl_4 \cdot H_2O$: in CH_3CN (20%)/CH_3OH, 304, 4.34; 281, 3.69; 273, 3.52; 264, 3.28; 261, 3.11; 256, 2.95; 245, 2.72; 232, 2.48; in acetone, 307, 3.57; 295, 3.33; 287, 3.14; 280, 2.89; 270, 2.63; 260, 2.43; 250, 2.14; 239, 1.95; 227, 1.54.

$[Fe((py)bimH)_3](BPh_4)_2 \cdot 3H_2O$: in CH_3CN (20%)/CH_3OH, 304, 5.55; 281, 5.12; 273, 5.08; 264, 4.91; 261, 4.70; 256, 4.59; 245, 4.32; 232, 3.92; in acetone, 312, 5.14; 297, 4.85; 285, 4.71; 278, 4.62; 270, 4.41; 260, 4.04; 250, 3.73; 243, 3.51; 234, 3.07; 226, 2.81; 218, 2.42.

Results and Discussion

Synthesis and Characterization. The two iron(II) complexes $[Fe((py)imH)_3]^{2+}$ and $[Fe((py)bim)_3)]^{2+}$ [4,17,18,23-25] and the deprotonated iron(III) complex $Fe((py)im)_3$[4] have been previously reported, but modified preparations for the BPh_4^- salts of the iron(II) compounds are given here. The neutral iron(III) complex has been prepared by deprotonation of the corresponding iron(II) tris complex via an intermediate compound whose elemental analysis is consistent with the bis species $Fe((py)imH)_2Cl_2$ (see Experimental Section). Analytical and conductivity results characterizing the tris iron(II) complexes, used in these studies, as monomeric 2:1 electrolytes and the tris iron(III) complex as a neutral species in solution are documented in the Experimental Section. In addition, the neutral $Fe((py)im)_3$ complex exhibits a parent ion peak in the mass spectrum ($M_p^+ = 488$ amu), whereas the iron(II) BPh_4^- salts display only low-weight fragments of the cations.

In their tris complexes with iron(II), the bidentate (py)imH and (py)bimH ligands are thought to coordinate through the pyridine and unsaturated imidazole (or benzimidazole) nitrogen as shown in Figure 1 for $[Fe((py)imH)_3]^{2+}$. Although no crystal structural information is yet available to distinguish between the *fac* and *mer* geometrical isomer possibilities for these tris complexes, solid-state infrared and magnetically perturbed Mössbauer data suggest the sterically less strained *mer* isomer is present in the solid state.[17] Crystal structure studies presently in progress on the ^1A and ^5T spin-state forms of the iron(II) complexes[26] should resolve this isomer question, as well as provide structural information on the spin-state-dependent ⟨Fe–ligand⟩ bond distance changes like those which are known to accompany spin conversion in other variable-spin iron(II)[27,28] and iron(III)[14,29] complexes.

Even though lattice solvation effects are not crucial for the solution-phase studies reported below, it is still interesting that our preparations yield solvates different from any yet published. The trihydrate of $[Fe((py)imH)_3](BPh_4)_2$ that Underhill et al.[25] isolated by precipitation by $NaBPh_4$ from

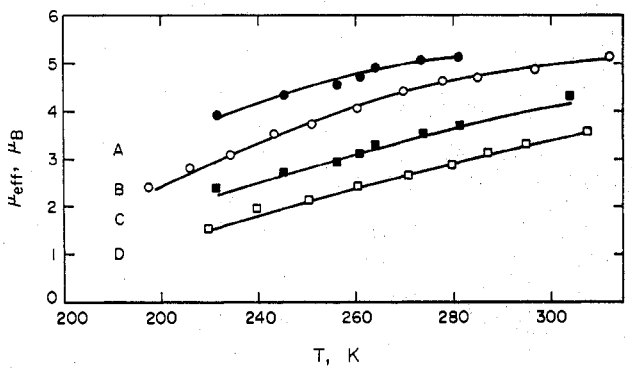

Figure 2. μ_{eff} vs. T plots characterizing the $^1A \rightleftarrows {}^5T$ equilibria in solution for (A) [Fe((py)bimH)$_3$](BPh$_4$) in CH_3CN (20%)/CH_3OH, (B) [Fe((py)bimH)$_3$](BPh$_4$) in acetone, (C) [Fe((py)imH)$_3$](BPh$_4$) in CH_3CN (20%)/CH_3OH, and (D) [Fe((py)imH)$_3$](BPh$_4$) in acetone.

ethanol (2.62 μ_B at 293 K) differs from the $CCl_4 \cdot H_2O$ solvate we obtained by precipitation of the compound from CH_2Cl_2 with CCl_4 (2.23 μ_B at 298 K). Likewise, the monohydrate of [Fe((py)bimH)$_3$](BPh$_4$)$_2$ that Sams et al.[18] isolated by precipitation with NaBPh$_4$ in 95% ethanol (4.9 μ_B at 300 K) differs from the trihydrate we obtained via precipitation of the same compound from methanol (5.1 μ_B at 298 K). Such differences appear commonplace for these complexes, regardless of the anion present.

Spin-State Measurements in Solution. Variable-temperature magnetic data for the [Fe((py)imH)$_3$]$^{2+}$ and [Fe((py)bimH)$_3$]$^{2+}$ cations in acetone and CH_3CN (20%)/CH_3OH solution are listed in the Experimental Section. The compounds have been characterized in the CH_3CN/CH_3OH solvent mixture for use in the T-jump measurements and in acetone for purposes of comparison with other existing data.

The non-Curie magnetic behavior of the complexes are displayed in Figure 2 as μ_{eff} vs. T plots. At all temperatures the observed magnetic moments fall between the low-spin ($S = 0$) and high-spin ($S = 2$) limits of ~0–5.5 μ_B expected for six-coordinate iron(II). The observed pattern with μ_{eff} decreasing with temperature is similar to that found for other solution-phase iron(II) spin equilibrium processes,[6,28,31] and this, along with the variable-temperature electronic spectral and laser T-jump measurements (vide infra), firmly establishes the existence of a

$$^1A(ls, S = 0) \rightleftarrows {}^5T(hs, S = 2) \quad (2)$$

thermal spin equilibrium in solution for these complexes. Boggess and Martin[32] have also previously noted the presence of the equilibrium in D_2O for the [Fe((py)imH)$_3$]$^{2+}$ complex (3.4 μ_B at room temperature). Magnetic data for the deprotonated [Fe((py)im)$_3$] complex have not been as extensively investigated, since the compound is essentially low-spin iron(III) in both the solid (μ_{298} = 2.01 μ_B) and solution (μ_{293} = 2.23 μ_B in CH_2Cl_2) states.

Change in color with temperature (thermochromism) is generally associated with iron(II) and iron(III) spin equilibria.[33] Sams and Tsin[17] described such a change for [Fe((py)imH)$_3$](X)$_2 \cdot n$H$_2$O (X = Br$^-$, n = 0; X = NO$_3^-$, n = 1; X = ClO$_4^-$, n = 1, 2) in the solid state but also concluded that the lack of thermochromicity in methanol precluded such a spin-equilibrium process in solution.[17,18] While it is true that a color change with temperature for [Fe((py)imH)$_3$]$^{2+}$ in methanol is difficult to detect, the orange-to-red change with decreasing temperature in acetone is much more marked, and the change for [Fe((py)bimH)$_3$]$^{2+}$ in both methanol and acetone is clearer still. The source of this thermochromicity is shown in Figure 3 where the visible electronic spectrum of [Fe((py)imH)$_3$]$^{2+}$ in solution is found to be strongly temperature dependent. The nature of this dependency, with a 486-nm band increasing in intensity with decreasing temperature, parallels an increase in the mole fraction of the ls isomer, as evidenced by the above magnetic susceptibility data. With extinction coefficients ranging from 1000 to 5000, this mainly "low-spin band" is most likely charge transfer in origin. The [Fe((py)bimH)$_3$]$^{2+}$ complex exhibits a similar temperature-dependent band centered at 520 nm. In both cases, these high-intensity CT bands apparently obscure any d–d transitions. It is quite surprising that, even with the very large intensity change in Figure 3, the solution is only slightly thermochromic. Thus, visual thermochromicity checks for spin equilibria should be considered, at best, as only positive tests.

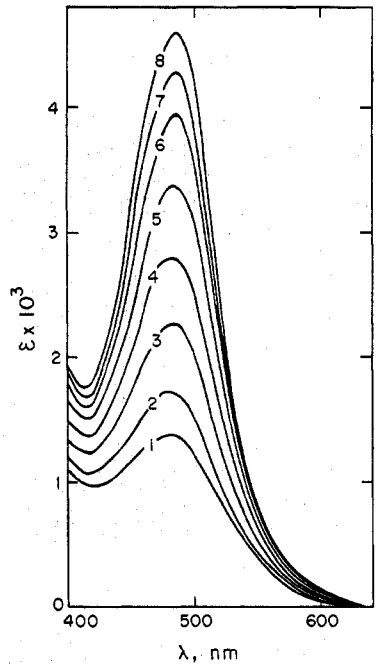

Figure 3. Variable-temperature electronic spectrum of [Fe((py)imH)$_3$](BPh$_4$) in CH_3CN (20%)/CH_3OH at (1) 302 K, (2) 296 K, (3) 285 K, (4) 207 K, (5) 265 K, (6) 254 K, (7) 246 K, and (8) 235 K.

Table I. Thermodynamic Parameters for the Iron(II) $^1A(ls) \rightarrow {}^5T(hs)$ Spin-Conversion Processes in Solution

Species	Solvent	$\Delta H°$,[a,b] kcal mol^{-1}	$\Delta S°$,[a,b] eu
[Fe((py)imH)$_3$]$^{2+}$	Acetone	3.8 (0.1)	11.6 (0.3)
	CH_3CN (20%)/CH_3OH	3.7 (0.2)	12.6 (0.4)
[Fe((py)bimH)$_3$]$^{2+}$	Acetone	4.7 (0.1)	18.6 (0.5)
	CH_3CN (20%)/CH_3OH	5.1 (0.4)	22.0 (1.7)

[a] Determined from magnetic susceptibility data (with standard deviation) assuming $K_{eq} = [{}^5T]/[{}^1A]$, $\mu_{eff}({}^5T) = 5.5$ μ_B, and $\mu_{eff}({}^1A) = 0$. [b] Calculated as described in ref 8.

By assuming ls and hs magnetic moments of 0 and 5.5 μ_B, respectively, equilibrium constants for the ls → hs processes may be determined from eq 3, and $\Delta H°$ and $\Delta S°$ thermodynamic parameters may be evaluated from the temperature

$$K_{eq} = [hs]/[ls] = (\mu^2_{exptl} - \mu^2_{ls})/(\mu^2_{hs} - \mu^2_{exptl}) \quad (3)$$

dependence of K_{eq}.[8,9] From the Figure 2 data, it is apparent that K_{eq}(bimH complex) > K_{eq}(imH complex) for a given set of temperature/solvent/anion conditions, implying that $10Dq_{((py)imH)_3} > 10Dq_{((py)bimH)_3}$. This seems reasonable because of the larger steric requirements of the (py)bimH ligand where larger *inter*ligand nonbonding interactions between the pyridine and benzimidazole rings would be expected to produce longer (and weaker) iron–nitrogen bonds and thus a smaller $10Dq$

Table II. Kinetic Parameters for Iron(II)

$$^1A(ls) \underset{k_{-1}}{\overset{k_1}{\rightleftharpoons}} {}^5T(hs)$$

Intersystem-Crossing Processes in Solution

Compd	Solvent (temp)	K_{eq}[a]	τ,[b] ns	k_1, s^{-1} [$\tau(^1A)$,[c] s]	k_{-1}, s^{-1} [$\tau(^5T)$,[c] s]	Ref
$[Fe(6\text{-Mepy})(py)_2tren](PF_6)_2$	Acetone (10%)/H_2O (20 °C)	0.05	120 (20)	4×10^5 [2.5×10^{-6}]	8×10^6 [1.3×10^{-7}]	7
$[Fe(6\text{-Mepy})_2(py)tren](PF_6)_2$	Acetone (10%)/H_2O (20 °C)	0.86	110 (30)	4×10^6 [2.5×10^{-7}]	5×10^6 [2×10^{-7}]	7
$Fe(HB(pz)_3)_2$	CH_3OH/CH_2Cl_2 (21 °C)	0.47	32 (10)	1×10^7 [1×10^{-7}]	2×10^7 [5×10^{-8}]	6
$[Fe((py)imH)_3](BPh_4)_2$	CH_3CN (20%)/CH_3OH (23 °C)	1.06	48 (8)	1.1×10^7 [9.1×10^{-8}]	1.0×10^7 [1.0×10^{-7}]	This work
	CH_3CN (20%)/CH_3OH (−2 °C)	0.59	45 (9)	8×10^6 [1.3×10^{-7}]	1.4×10^7 [5.6×10^{-8}]	This work

[a] Equilibrium constant defined as $K_{eq} = [hs]/[ls]$. [b] First-order relaxation time; error in τ (±ns) reflects the range of values obtained from at least six lasings of the same sample. [c] Spin-state lifetime: $\tau(\text{spin state}) = k^{-1}$.

value. Similar ligand steric interactions are also known to induce and "fine tune" $^1A \rightleftarrows {}^5T$ spin crossover in the $[Fe(2\text{-Mephen})_3]^{2+}$ and $[Fe(6\text{-Mepy})_n(py)_m tren]^{2+}$ complexes.[28,34]

The $\Delta H°$ and $\Delta S°$ thermodynamic parameters in solution for the ls → hs conversions are given in Table I. The $\Delta H°$ parameters, which range from 3.7 to 5.0 kcal mol^{-1}, are similar to those found for the bis[hydrotris(1-pyrazolyl)borate]iron(II) $[Fe(HB(pz)_3)_2]$ (3.9 kcal mol^{-1} in acetone)[30] and $[Fe(6\text{-Mepy})(py)_2tren]^{2+}$ (4.6 kcal mol^{-1} in acetone)[28] compounds. Qualitatively, these $\Delta H°$ values reflect the changing ⟨metal–ligand⟩ bond distances and energies which occur upon ls → hs conversion. In fact, it has recently been shown[12,13] that for reasonable bond distance changes of 0.10–0.20 Å E_r, the inner coordination sphere reorganization energy, would be expected to be 2.0–6.0 kcal mol^{-1}. Thus, inner-sphere reorganization appears to provide the dominant enthalpic term in these and probably all other spin-equilibrium processes. The $\Delta S°$ values in Table I contain an "electronic entropy" change due to differences in spin multiplicity and state degeneracy for the ls and hs forms. For $^1A(ls) \rightarrow {}^5T(hs)$ conversion, $\Delta S°$ (electronic) = 5.2 eu (from R ln 15). However, since the microsymmetry of the $[Fe((py)imH)_3]^{2+}$ and $[Fe((py)bimH_3]^{2+}$ cations can effectively be no greater than D_3, the molecules are at least trigonally distorted so that $^5T(O_h) \rightarrow {}^5E + {}^5A$ and the actual spin conversion is either $^1A(ls) \rightarrow {}^5E(hs)$ for which $\Delta S°$(electronic) = 4.6 eu or $^1A(ls) \rightarrow {}^5A(hs)$ where $\Delta S°$(electronic) = 3.2 eu. For the $Fe(HB(pz)_3)_2$ and $[Fe(6\text{-Mepy})_3tren]^{2+}$ complexes, the trigonal distortion parameter is ~1000 cm^{-1} and the actual spin equilibria have been analyzed as $^1A(ls) \rightarrow {}^5A(hs)$ cases.[7,30] The remaining and dominant $\Delta S°$ terms in Table I probably arise from spin-change-induced outer-sphere reorganization of the solvent cage. Thus, some solvent dependency on $\Delta S°$ is not surprising. In this regard, it is interesting to note that the present spin equilibria possess some of the largest $\Delta S°$ parameters found to date for Fe(II) processes, indicating that solvation effects may be more important for these than for the other complexes in determining the relative stabilities of the two spin states. In fact, $\Delta S°$ is found to be 26.8 (0.7) for the $[Fe((py)imH)_3]^{2+}$ compound in pure CH_3CN which is the largest value yet measured for *any* ls → hs solution process. The source of such a large entropic term is not certain; however, the backside N–H imidazole proton offers an inviting site for solvent···HN hydrogen-bonding interactions which, if strongly spin-state dependent, could promote an exceptionally large solvent-sphere reorganization upon spin conversion.

A large spin-state-specific change in the visible spectrum with temperature for metal complexes undergoing thermal spin equilibria lends itself well to direct measurement of the intersystem crossing kinetics using the laser Raman temperature-jump method. The application of the technique for this purpose has been discussed elsewhere.[6,7,13] The experimental conditions and methods used in this work to determine k_1 and k_1 (see eq 4) for $[Fe((py)imH)_3]^{2+}$ are given in the Experi-

$$^1A(ls) \underset{k_{-1}}{\overset{k_1}{\rightleftharpoons}} {}^5T(hs) \tag{4}$$

mental Section. By monitoring the temperature-dependent transmittance change at 486 nm with time (ns), spin-relaxation traces were obtained on a storage oscilloscope and the data analyzed by both (1) a nonlinear least-squares fit of the data to eq 5, thus allowing for the adjustment of T_0 (transmittance

$$T = T_\infty + (T_0 - T_\infty)\exp(-(t - t_0)/\tau) \tag{5}$$

at t_0) and especially T_∞ (transmittance at t_∞) in converging to the "best" estimate for the first-order relaxation time, τ,[35] and (2) application of the "second" method-of-moments equation to the derivative of the relaxation traces.[36] The latter method has been found indispensable for especially "rapid" spin-relaxation processes[11,12] where $\tau \lesssim 30$ ns approaches the limit of the laser heating pulse width of ~25 ns. In the present case, with $\tau > 30$ ns, the method-of-moments approach, while not required, has also been employed as an alternate data treatment procedure. Application of eq 5 to the $[Fe((py)imH)_3]^{2+}$ relaxation traces (Table II, footnote *b*) yields τ = 48 ns at 23 °C and τ = 45 ns at −2 °C, while for the method-of-moments approach, τ = 46 ns (23 °C). The lack of a strong temperature dependency on τ, for the available temperature range, does not appear to be an unusual feature of spin-interconversion processes, in general.[7,12,13]

Intersystem-crossing kinetic data for the present $[Fe((py)imH)_3]^{2+}$ complex and data for the only other two $^1A(ls) \rightleftarrows {}^5T(hs)$ systems thus far investigated are summarized in Table II. Clearly, the cationic tris bidentate $[Fe((py)imH)_3]^{2+}$ species and the neutral bis tridentate $Fe(HB(pz)_3)_2$ complex exhibit essentially indistinguishable intersystem crossing kinetics, whereas the cationic hexadentate-ligated $[Fe(6\text{-Mepy})_n(py)_m tren]^{2+}$ compounds exhibit some of the "slowest" kinetics yet measured for a spin-equilibrium process, regardless of metal ion or oxidation state.[13] This finding lends further support to the view[7,12-14] that chelated multidentate ligands, such as $(6\text{-Mepy})_n(py)_m tren$ may act to retard spin interconversion by offering "mechanical restrictions" to the inner-sphere reorganization process which must occur upon ls ⇄ hs conversion. For the $[Fe(6\text{-Mepy})_n(py)_m tren]^{2+}$ complexes, x-ray crystallographic studies indicate *intra*ligand restrictions of this nature could arise from nonbonding interactions between methylene protons on the tren backbone or methyl group–pyridine ring steric interactions in one of the

polyhedral faces.[7,28] Molecular models indicate no similar stereochemical restrictions to structural change in either the $Fe(HB(pz)_3)_2$ or $[Fe((py)imH)_3]^{2+}$ species.

Acknowledgment. Support of this work by the National Science Foundation, the Robert A. Welch Foundation under Grant C-627, and the donors of the Petroleum Research Fund, administered by the American Chemical Society, is gratefully acknowledged. E.V.D. also thanks the Energy Research and Development Agency for a summer fellowship and travel grant (Grant T-179) to Brookhaven National Laboratory as administered under the auspices of the Associated Universities Program. We especially thank Drs. Mitchell Hoselton and Norman Sutin for the kind availability of and assistance with the laser *T*-jump apparatus and for many enlightening comments and rewarding discussions during the course of the work.

Registry No. $[Fe((py)imH)_3]^{2+}$, 65494-05-5; $[Fe((py)bimH)_3]^{2+}$, 58957-72-5; (py)imH, 18653-75-3; $[Fe((py)imH)_3](BPh_4)_2$, 65494-06-6; $[Fe((py)bimH)_3](BPh_4)_2$, 58957-75-8; $Fe((py)im)_3$, 65494-04-4.

References and Notes

(1) Rice University Predoctoral Fellow.
(2) Robert A. Welch Predoctoral Fellow; ERDA Predoctoral Fellow, Summer 1976, at Brookhaven National Laboratory.
(3) L. Cambi and L. Szego, *Ber. Dtsch. Chem. Ges.*, **64**, 2591 (1931).
(4) B. Chiswell, F. Lions, and B. S. Morris, *Inorg. Chem.*, **3**, 110 (1964).
(5) D. M. L. Goodgame and A. A. S. C. Machado, *Inorg. Chem.*, **8**, 2031 (1969).
(6) J. K. Beattie, N. Sutin, D. H. Turner, and G. W. Flynn, *J. Am. Chem. Soc.*, **95**, 2052 (1973).
(7) M. A. Hoselton, R. S. Drago, L. J. Wilson, and N. Sutin, *J. Am. Chem. Soc.*, **98**, 6967 (1976).
(8) M. F. Tweedle and L. J. Wilson, *J. Am. Chem. Soc.*, **98**, 4824 (1976).
(9) E. V. Dose, K. M. M. Murphy, and L. J. Wilson, *Inorg. Chem.*, **15**, 2622 (1976).
(10) M. G. Simmons and L. J. Wilson, *Inorg. Chem.*, **16**, 126 (1977).
(11) E. V. Dose, M. F. Tweedle, L. J. Wilson, and N. Sutin, *J. Am. Chem. Soc.*, **99**, 3886 (1977).
(12) R. H. Petty, E. V. Dose, M. F. Tweedle, and L. J. Wilson, *Inorg. Chem.*, in press.
(13) E. V. Dose, M. A. Hoselton, N. Sutin, M. F. Tweedle, and L. J. Wilson, *J. Am. Chem. Soc.*, in press.
(14) E. V. Dose, G. Sim, E. Sinn, M. F. Tweedle, and L. J. Wilson, *J. Am. Chem. Soc.*, in press.
(15) See for example A. W. Adamson, *Adv. Chem. Ser.*, **No. 150**, 128–148 (1976).
(16) H. C. Stynes and J. A. Ibers, *Inorg. Chem.*, **10**, 2304 (1971).
(17) J. R. Sams and T. B. Tsin, *J. Chem. Soc., Dalton Trans.*, 488 (1976).
(18) J. R. Sams and T. B. Tsin, *Inorg. Chem.*, **15**, 1544 (1976).
(19) D. F. Evans, *J. Chem. Soc.*, 2037 (1959).
(20) D. Ostfeld and I. A. Cohen, *J. Chem. Educ.*, **49**, 829 (1972).
(21) D. H. Turner, G. W. Flynn, N. Sutin, and J. V. Beitz, *J. Am. Chem. Soc.*, **94**, 1554 (1972).
(22) B. Radziszewski, *Chem. Ber.*, **110**, 2706 (1977).
(23) T. R. Harkins, J. L. Walker, O. E. Harns, and H. Feiser, *J. Am. Chem. Soc.*, **78**, 260 (1956).
(24) T. R. Harkins and H. Feiser, *J. Am. Chem. Soc.*, **78**, 1143 (1956).
(25) R. J. Dosser, J. J. Eilbeck, A. E. Underhill, P. R. Edwards, and E. E. Johnson, *J. Chem. Soc. A*, 810 (1969).
(26) E. Sinn and L. J. Wilson, to be submitted for publication.
(27) E. Konig and K. J. Watson, *Chem. Phys. Lett.*, **6**, 457 (1970).
(28) M. A. Hoselton, L. J. Wilson, and R. S. Drago, *J. Am. Chem. Soc.*, **97**, 1722 (1975).
(29) B. F. Hoskins and C. D. Panna, *Inorg. Nucl. Chem. Lett.*, **11**, 409 (1975).
(30) J. P. Jesson, S. Trofimenki, and D. R. Eaton, *J. Am. Chem. Soc.*, **89**, 3158 (1967).
(31) L. J. Wilson, D. Georges, and M. A. Hoselton, *Inorg. Chem.*, **14**, 2968 (1975).
(32) R. K. Boggess and R. B. Martin, *Inorg. Chem.*, **13**, 1525 (1974).
(33) K. R. Kunze, D. L. Perry, and L. J. Wilson, *Inorg. Chem.*, **16**, 594 (1977), and references therein.
(34) H. A. Goodwin and R. N. Sylva, *Aust. J. Chem.*, **21**, 83 (1968).
(35) The use of transmittance directly in place of the absorbance of the sample (which is normally used) is valid for cases where the change in absorbance is small, as is true for these samples undergoing a small (1–3 °C) temperature perturbation. The function minimized was $\sum(T_{obsd} - T_{calcd})^2$.
(36) S. S. Brody, *Rev. Sci. Instrum.*, **28**, 1021 (1957); D. H. Cooper, *ibid.*, **37**, 1407 (1966).

Contribution from the Department of Chemistry, The University of Texas at Austin, Austin, Texas 78712

Ground States of Molecules. 46.[1] MNDO Study of Hydroboration of Alkenes and Alkynes

MICHAEL J. S. DEWAR* and M. L. McKEE

Received July 6, 1977

MNDO calculations are reported for the reactions of borane with ethylene, propene, isobutene, vinyl chloride, vinyl fluoride, acetylene, and methylacetylene and of methylborane and dimethylborane with propene. The results are consistent with the available evidence and indicate that the orientation of addition to olefins is determined primarily by steric effects. Addition to vinyl chloride is predicted to take place with Markownikoff orientation but to vinyl fluoride with anti-Markownikoff orientation.

Introduction

In the 20 years since Brown and Rao[2] first reported addition of boranes to olefins, such hydroboration reactions have become of major importance in organic synthesis.[3-6] Olefins of all types react rapidly with BH_3, even if the double bond is highly hindered. If hindrance is low, the reaction proceeds further to a trialkylborane. If bulky substituents are present, the reaction may stop at the monoalkyl- or dialkylborane stage.

Hydroboration is usually carried out in ethereal solution, using an ether–borane complex as the source of BH_3. Tetrahydrofuran has been found especially suitable. Under these conditions addition to unsymmetrically substituted ethylenes leads to predominant anti-Markownikoff addition,[4-6] mono-*n*-alkyl derivatives giving tri-*n*-alkylboranes in which ca. 94% of the alkyl groups are attached to boron through C_1, the rest through C_2. This selectivity refers to an average over the three successive hydroborations leading to the final product. In more hindered cases, essentially 100% of one product can be obtained.

The role of the solvent is still uncertain. In ethers such as tetrahydrofuran, borane exists as a complex,[7] $R_2O \rightarrow BH_3$. This might react directly with the olefin, or it may first have to dissociate into its components. In the latter case, the dissociation may be reversible or rate determining. Pasto et al.[8] have concluded on the basis of kinetic studies that the eth-

0020-1669/78/1317-1075$01.00/0